Review of Scientific Instruments

RESEARCH ARTICLE | JULY 17 2024

Impedance-matched coplanar-waveguide metal-powder low-pass filters for cryogenic applications

Matvey Lyatti ; Raphael Roth; Irina Gundareva ; Detlev Grützmacher ; Thomas Schäpers

Rev. Sci. Instrum. 95, 074708 (2024)
https://doi.org/10.1063/5.0184242

Review of Scientific Instruments ARTICLE pubs.aip.org/aip/rsi

Impedance-matched coplanar-waveguide metal-powder low-pass filters for cryogenic applications

Cite as: Rev. Sci. Instrum. 95, 074708 (2024); doi: 10.1063/5.0184242
Submitted: 25 October 2023 • Accepted: 24 June 2024 •
Published Online: 17 July 2024

Matvey Lyatti,[1,2,a] Raphael Roth,[1,2] Irina Gundareva,[1,2] Detlev Grützmacher,[1,2] and Thomas Schäpers[1,2]

AFFILIATIONS

[1] Peter Grünberg Institut (PGI-9), Forschungszentrum Jülich, 52425 Jülich, Germany
[2] JARA-Fundamentals of Future Information Technology, Jülich-Aachen Research Alliance, Forschungszentrum Jülich and RWTH Aachen University, Jülich, Germany

[a] Author to whom correspondence should be addressed: m.lyatti@fz-juelich.de

ABSTRACT

We developed impedance-matched metal-powder low-pass filters based on coplanar waveguide design and characterized them at room temperature and 77.4 K. The coplanar waveguide metal-powder (CPW-MP) filters have a return loss better than 9.8 dB at frequencies up to 10 GHz at 77.4 K. We find that the filter attenuation per length scales linearly with frequency from 29 to 220 dB/m within the 1–5 GHz frequency range at 77.4 K, achieving the total attenuation above 100 dB for the 1 m-long CPW-MP filter at frequencies above 2 GHz. The CPW-MP filter integrated with the multipole LC filter demonstrates the low cut-off frequency, the attenuation above 100 dB in the stop band, and the high roll-off of 590 dB per decade. The proposed CPW-MP filter is easy to fabricate, has very good thermal-shock resistance, is flexible for integration with other types of low-pass filters, delivers the same performance as classical cryogenic filters, is more compact compared to 50 Ω coax cables with the same type of lossy dielectric, and provides ample opportunities for further miniaturization.

I. INTRODUCTION AND MOTIVATION

Broadband low-frequency filters are an integral part of cryogenic measurement setups. They provide appropriate attenuation and thermalization of the transmission lines connecting room-temperature equipment and the device under test to keep its electronic temperature close to the base temperature of the cryogenic refrigerator. Ideally, the electromagnetic spectrum of the low-pass filter output has to be equal to that of the blackbody radiation at the lowest temperature of the sample. The frequency bandwidth of such a filter has to significantly exceed the frequency bandwidth of the transmission line to fulfill this requirement. The filter bandwidth requirement imposes restrictions on the applicability of many types of low-pass filters, as they are effective over a limited frequency bandwidth. The metal powder (MP) filters, first discussed by Martinis *et al.*,[1] are perhaps the most popular type of cryogenic filters because of their simple design, high attenuation, and large frequency bandwidth that exceeds the bandwidth of the typical transmission lines used in cryogenic setups. The conventional MP filter consists of a central conductor surrounded by metal powder or a metal powder/epoxy mixture.[2] The filter attenuates an incoming electrical signal via eddy current dissipation in the metal powder. The central conductor in such a filter is shaped into the form of a spiral or meander for both high attenuation and compact size.[2–5] The different types of cryogenic low-pass filters were reviewed and compared by Bladh *et al.*[6] and Thalmann *et al.*[7]

In many applications, e.g., in rf reflectometry measurements,[8,9] it is necessary to have an all-impedance-matched measurement setup. There are a few types of impedance-matched MP low-pass filters. One of these is the lossy coax cable.[4,10–16] Another one utilizes the strip line design.[7,17] The design and parameters of impedance-matched absorbing low-pass filters are presented in Table I. The first coax cable filters used MgO, polyamide, or metal powder-filled

TABLE I. Comparison of different impedance matched absorptive low-pass filters. The attenuation at a frequency of 2 GHz is estimated as the difference between the attenuation at a frequency of 2 GHz and zero frequency.

Approach	Impedance matched	Dielectric	Return losses	Attenuation per unit length at 2 GHz (dB/m)	References
Coax cable	Yes	MgO	n.a. Z = 17 Ω	75	10
Microcoax cable	Yes	Polyimide	n.a. Z = 53 Ω	84	11
Coax cable	Yes	Bronze powder/epoxy	n.a. Z = 53–71 Ω	100	4
Coax cable	Yes	Metal powder/epoxy	>11 dB at f ≤ 50 GHz	55	12
Coax cable	Yes	Eccosorb CR-124	>10 dB at f ≤ 20 GHz	740–980	13
Coax cable	Yes	Esorb-230	>10 dB at f ≤ 43 GHz	230	14
Coax cable	Yes	Eccosorb CR-110	>20 dB at f ≤ 40 GHz	50	15
Coax cable	Yes	Carbon nanotubes	>8 dB at f ≤ 45 GHz	690–2700 dB at f = 3.6 GHz	16
Stripline	Yes	Eccosorb CR-124	>10 dB at f ≤ 40 GHz	980	17
Stripline on FR4 PCB	Yes (intermediate device)	Soft ferrite/silicone rubber	n.a.	540	7
Differential meander line on FR4 PCB	No	Stainless steel powder/epoxy	n.a.	70	3
Coplanar waveguide on FR4 PCB	Yes	Stainless steel powder/GE varnish	>9.8 dB at f ≤ 10 GHz	75	This work

epoxy as a lossy dielectric. These coax cable filters have an attenuation per cable length of 64–110 dB/m, as listed in Table I, which requires meter-long cables to get attenuation above 100 dB in the GHz frequency range. The use of magnetically loaded dielectrics has made it possible to significantly reduce the coax cable filter length because of the larger attenuation per cable length, up to 980 dB/m in the case of the Eccosorb CR-124 dielectric. The efficiency of some magnetically loaded dielectrics was tested at frequencies up to 110 GHz.[14] The attenuation of the stripline filters with magnetically loaded dielectric demonstrated the same performance as the coax cable filters (see Table I). As can be seen from the table, the attenuation per unit length mainly depends on the type of absorption coating. Thus, the investigation of filter design based on planar structures is of interest because the size of such filters can be reduced using lithographic methods while maintaining the same characteristic impedance.

In this article, we present fabrication details and characterization of a novel type of impedance-matched metal powder filter based on a coplanar waveguide (CPW) design. We integrate this filter with a multipole LC filter for the low cut-off frequency. These filters are easy to fabricate and provide great opportunities for miniaturization.

II. FILTER FABRICATION

Filter fabrication steps are shown in Fig. 1. The CPW is patterned on a two-sided printed circuit board (PCB) made of FR4 dielectric with a dielectric constant of 4.5 and covered with 35 μm thick copper from both sides. We soldered the CPW input and output to the edge mount SubMiniature version A (SMA) connectors, as shown in Fig. 1(a), to investigate the filter characteristics at high frequencies. The top side of the PCB with CPW is covered with a 2.5 mm thick microwave absorption coating made of 22–53 μm spherical-shape non-magnetic stainless steel powder St. 1.3964 mixed with VGE-7031 varnish (Lake Shore Cryotronics).[18] The VGE-7031 varnish was diluted with ethanol in a volume proportion of 1:3 to achieve a high filling ratio for the absorption coating. The VGE-7031 varnish is an electrical insulator with a resistivity

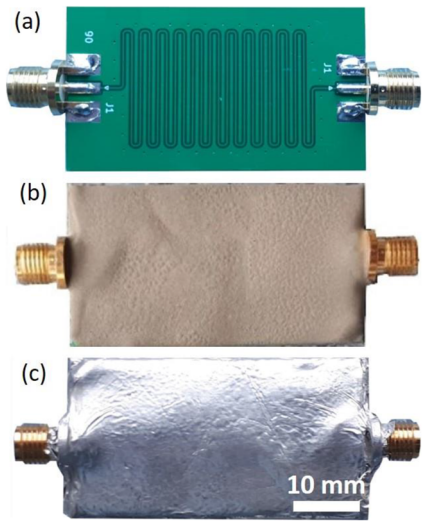

FIG. 1. Fabrication of the low-frequency coplanar waveguide metal powder filter. (a) PCB with CPW connected to the SMA connectors. (b) PCB board covered with metal powder absorption coating. (c) PCB board with metal powder absorption coating shielded with self-adhesive aluminum foil.

$>1 \times 10^{15}$ Ω m. The diluted varnish was added to the stainless steel powder until a thin layer of varnish was formed atop it, indicating that all the gaps between the stainless steel particles were filled. The ready-to-use mixture has the consistency of wet sand. The applied stainless-steel powder/VGE varnish coating was cured in the oven at 70 °C for 1 h. The CPW filter covered with the absorption coating is shown in Fig. 1(b). The dc resistance of the filter measured between the central track and the ground is well above the 100 MΩ measurement limit of the multimeter HP34401A.

In contrast to the MP absorption coating with the epoxy resin "Loctite Stycast 2850FT BL" binder, the MP/VGE varnish coating has a higher filling rate and can be easily removed with ethanol, which makes it possible to modify or repair the manufactured filters. At the prototyping stage, we wrapped the filter with self-adhesive aluminum foil, as shown in Fig. 1(c), to reduce the input–output (I/O) cross-talk. The self-adhesive aluminum foil has a conductive glue that provides good electrical contact between the PCB ground plane and the aluminum foil. In the final design, the PCB is placed into a gold-plated copper housing that can be mounted on the cryostat cold plate, as discussed below.

III. RESULTS AND DISCUSSION

A. Return losses

The cross section of the CPW-MP filter is schematically shown in Fig. 2(a). Here, the track width is denoted as W, the gap between the track and the side ground electrodes as S, and the distances from the track to the bottom and top ground electrodes as d_1 and d_2, respectively. When $S \ll d_1$ and d_2, the characteristic impedance of CPW sandwiched between two dielectrics depends mainly on the track width W, the gap between the track and side ground electrodes S, and the dielectric constants ε_1 and ε_2 of the bottom and top dielectrics.[19] The 10 μm-thick solder mask with a dielectric constant of $\varepsilon_{SM} = 3.8$ is not shown in Fig. 2(a). The thickness of the solder mask is significantly smaller than the d_1, d_2, and S values, and the dielectric constant of the solder mask is smaller than the dielectric constants ε_1 and ε_2 of the bottom and top dielectrics.[20] Therefore, the contribution of the solder mask to the CPW characteristic impedance is small.

Since the dielectric constant of the stainless steel absorption coating is unknown, we fabricate a series of straight 50 mm-long CPWs with a "nominal" characteristic impedance without the absorption coating ranging from 50 to 120 Ω, cover them with the stainless steel absorption coating, and measure their return loss (S11 parameter) in the 10 MHz to 10 GHz frequency range using the ZNB vector-network analyzer (VNA) from Rohde and Schwarz. The CPWs were connected to the VNA with two 0.57 m-long semi-flexible coax cables. The signal path calibration was performed at room temperature using the calibration unit ZN-Z53 (Rohde and Schwarz). The measurement results at room temperature (293 K) for three CPWs with the "nominal" characteristic impedance of 81.5, 89.2, and 100.8 Ω are presented in Fig. 2(b). The values of the characteristic impedances were calculated with Advances Design Studio 2024 (ADS2024) (Keysight). The best impedance matching to 50 Ω coax cables over the whole frequency range up to 10 GHz is achieved for the CPW with the "nominal" characteristic impedance of 89.2 Ω [dark gray line in Fig. 2(b)]. The S11 parameter of the 89.2 Ω CPW at frequencies up to 550 MHz, where the reflectivity measurements are carried out,[8,9] is above 20 dB so that less than 1% of the incident power is reflected from the CPW. In the broader frequency range up to 10 GHz, which is of interest, e.g., for qubit measurements, the S11 parameter of the 89.2 Ω CPW is below −10.3 dB, indicating a good impedance match. Since the possibility of fabricating multichannel filters is one of the advantages of the proposed design, the crosstalk between separate channels placed on the same PCB becomes an important parameter. We measured the cross-talk between the neighboring 50 mm-long CPWs placed on the same PCB 15 mm apart (see the supplementary material for the cross-talk measurement description) and found that it was below −50 dB at frequencies up to 10 GHz.

Using ADS2024, we estimate the effective dielectric constant of the CPW with the stainless steel powder/VGE varnish coating as

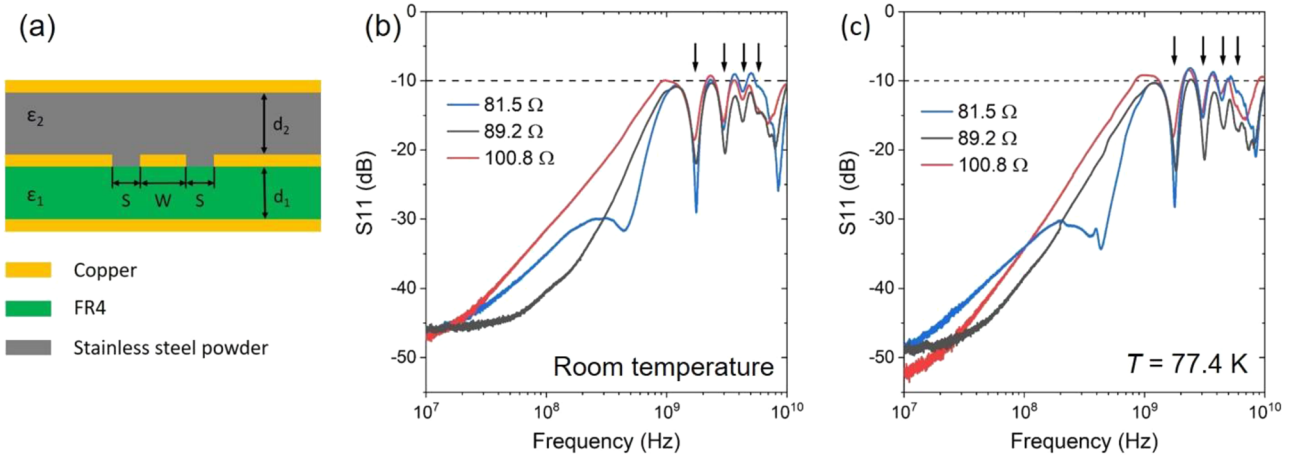

FIG. 2. (a) The cross section of the CPW filter. S11 parameter of the CPW-MP filters with various "nominal" characteristic impedances at (b) room temperature and (c) $T = 77.4$ K. The black dashed lines show a −10 dB level. Black arrows show the positions of the geometric resonances in the CPW.

ε_{eff} = 8.1 and the dielectric constant of the stainless steel powder/VGE varnish absorption coating as ε_s = 11.7. Comparing the ε_s value with a theoretical value of 12.4 for the stainless steel metal powder with a particle size of 44 μm and a density of 48%, we conclude that we achieved a high filling ratio for the MP/VGE varnish absorption coating.[21] Here, one should take into account that the maximum theoretical density for the spherical particle packing is equal to 74%.

The frequency dependences of the S11 parameter possess a series of dips, shown in Fig. 2(b) by black arrows, due to geometric resonances in the CPW.

Since Mueller *et al.*[3] reported that the PCB-MP filters demonstrate nearly identical behavior in the 10 mK to 77 K temperature range, we measured the low-temperature performance of the CPW-MP filters at 77.4 K by immersing them in liquid nitrogen. We did not perform the separate signal path calibration at T = 77.4 K but instead checked the validity of the room-temperature calibration by measuring the S11 parameter of the SMA female to SMA female adapter immersed in liquid nitrogen. The S11 parameter of the SMA female to SMA female adapter was nearly unchanged at frequencies below 10 GHz (see the supplementary material). The frequency dependences of the S11 parameter at the temperature T = 77.4 K are presented in Fig. 2(c). As for the room-temperature measurements, the best impedance matching was achieved for the 89.2 Ω CPW. The S11 parameter at T = 77.4 K is only slightly smaller compared to room temperature measurements due to the more pronounced resonances. The S11 parameter at T = 77.4 K is better than −20 dB at frequencies up to 470 MHz and below -9.8 dB at frequencies up to 10 GHz, demonstrating good impedance matching with 50 Ω coax cables. From the above experimental results, we conclude that CPW with the stainless steel powder/VGE varnish absorption coating can be used for impedance-matched broadband cryogenic low-pass filters.

B. Attenuation

When the gap S between the track and the ground electrodes is smaller than the distances between the track and the top and bottom ground electrodes, the electric field is mainly confined in the gaps between the track and the side ground electrodes of CPW. Therefore, it can be efficiently coupled to the absorption coating, especially when the dielectric constant of the absorption coating is higher than the dielectric constant of the PCB. Since the attenuation of the MP filters depends on the wire length, one needs to know the attenuation per unit length in the frequency range of interest to design the low-pass filter matching the experiment requirements.

We fabricated four CPW-MP filters using the "89.2 Ω" design, which provides the best impedance match. The filters have a central track length L of 0.11 (A), 0.207 (B), 0.305 (C), and 0.408 (D) m. The PCBs have a length and width of 45 and 25 mm, respectively. The central track of CPW was folded into a meander to reduce the length of the filter, as shown in Fig. 1(a). The filters were connected to the VNA by two 0.57 m-long semiflexible coax cables.

The S11 parameters of the filter C measured at room temperature and at T = 77.4 K are shown in Fig. 3(a). Similar to the 50 mm-long CPW-MP filter discussed in section A, filter C has an S11 parameter better than −10 dB at frequencies below 10 GHz. The geometrical resonances are shifted to the lower frequencies because of the longer central track. We measured the S12 parameter of individual filters and their series connections to determine the attenuation of CPW-MP filters per unit length. Twelve S12 curves were acquired for the CPW-MP filters, with the total length varying from 0.11 to 1.03 m. The frequency dependence of the S12 parameter of the CPW-MP filters with the selected lengths measured at room temperature is shown in Fig. 3(b). The attenuation of the single filter [dark gray line in Fig. 3(b)] is limited at high frequencies to ~60 dB by the I/O cross talk. When the filters are connected in series, the (I/O) cross talk is eliminated, and the attenuation at high frequencies exceeds 100 dB. Alternatively, the I/O cross talk can be reduced by splitting the PCB in two or by making appropriate cuts in the PCB. The attenuation at the fixed frequency, as expected, scales exponentially with the CPW length. We determined the attenuation per unit length at fixed frequencies from the linear fit of the S12(L) dependence and plotted it in the inset of Fig. 3(a). The experimental points with attenuation close to the VNA noise floor were excluded

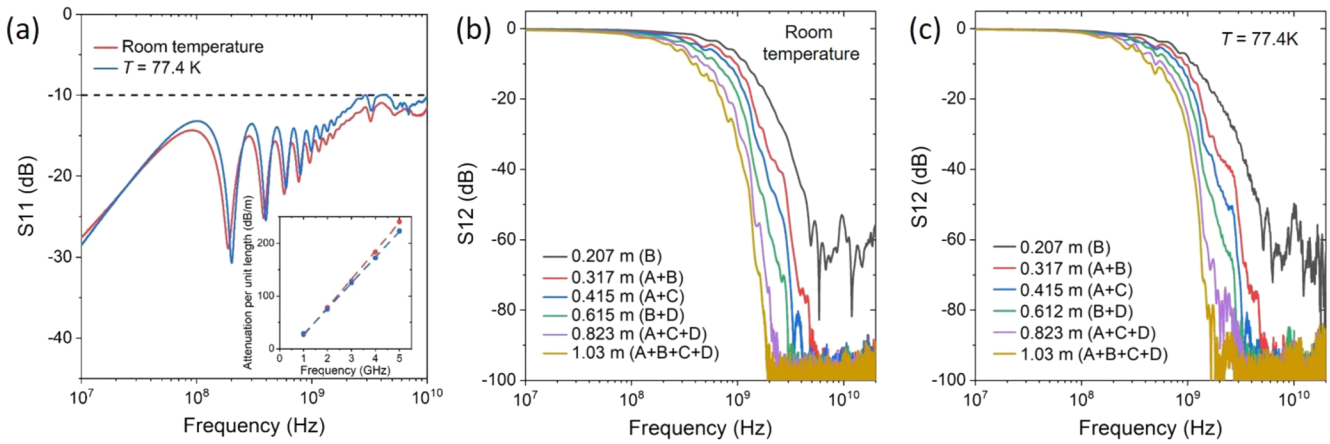

FIG. 3. (a) S11 parameter of the CPW-MP filter with a central track length of 0.305 m. The inset shows the attenuation per length at different frequencies at room temperature (red points) and T = 77.4 K (blue points). Dashed lines are a linear fit. S12 parameter of the CPW-MP filter of various lengths at (b) room temperature and (c) 77.4 K.

from the linear fit. The attenuation per unit length depends linearly on the frequency within the 1–5 GHz frequency range, reaching a value of 240 dB/m at 5 GHz. The red dashed line shows a linear fit of the experimental data. The same measurements were performed at T = 77.4 K. The S12 parameters of the filters are shown in Fig. 3(c). The attenuation per unit length was only slightly reduced compared with room-temperature measurements, as shown in the inset of Fig. 3(a).

To get a higher attenuation, we used the PCB design with rather sparse stitching, as shown in Fig. 1(a). The dense via stitching typically improves the high-frequency performance of the CPW. Trying to improve the filter performance, we fabricated the same PCBs using a 1 mm step via stitching and found no improvement in the S11 parameter, but the attenuation at frequencies above 4 GHz was reduced by about 20%. Therefore, we conclude that the sparse stitching is favorable for higher attenuation.

The measured attenuation per unit length is comparable to that of the conventional coax cable and PCB filters, which use the same type of absorption coating (see Table I). The CPW-MP filter has no loops, which reduces magnetic field pick-up. The size of the CPW-MP filters discussed in this section is limited by the capabilities of the PCB manufacturer, which defines the minimum trace width as 0.127 mm. Since the characteristic impedance of the CPW-MP filter depends on the widths of the central track and gaps between the central track and side ground planes, the size of the filter can be reduced by a factor of ten, if required, using lithography techniques.

C. Integration with multistage LC filter

The cut-off frequency of the powder filters can be significantly decreased with the LC filters, as shown by Lukashenko and Ustinov.[2] The proposed CPW-MP filter can be easily integrated with the LC filter by connecting the CPW central track to the side ground plane by surface-mount device (SMD) capacitors, as shown in the inset of Fig. 4(a). To study the performance of the CPW-MP filter integrated with the LC filter, we fabricated: (LC-A) the 0.113 m-long CPW integrated with a one-pole π-type LC filter; (LC-B) the 0.214 m-long CPW integrated with a two-pole π-type LC filter; and (LC-C) the 0.314 m-long CPW integrated with a three-pole π-type LC filter shown in the inset in Fig. 4(a). The capacitance C of the LC filter is mainly defined by the capacitance of the SMD capacitor, and the inductance L is determined by the inductance of the CPW central track. The cut-off frequency of the LC filter can be modified by changing the capacitance of the SMD capacitors and the CPW dimensions. The 0603 SMD capacitors with a temperature-independent C0G dielectric from TDK were used.[22]

We chose 100 pF capacitors to fabricate the LC filters because their high frequency performance was good enough so that the stop-bands of the CPW-MP and LC filters overlapped, providing large attenuation at frequencies above the cut-off frequency of the LC filter. The attenuation of the series connection of the filters LC-A, LC-B, and LC-C with a total central track length of 0.641 m is shown in Fig. 4(a) by the red line. The series connection of the filters demonstrates the 3 dB attenuation at the frequency of 6.3 MHz and a very sharp decrease of the transmission from −10 to −100 dB in the 130–190 MHz frequency range, providing a roll-off of 590 dB per decade. The frequency at which the filter transmittance decreases sharply is close to the estimated cut-off frequency of $f_c = 1/2\pi(LC)^{1/2}$ = 100 MHz, where C = 100 pF and L = 26 nH is the inductance of the 100 mm-long CPW track between the capacitors. We attribute the small decrease in the attenuation at 1.5–2 GHz to the geometric resonance in the PCB. An increase in the CPW central-track length up to 0.848 m is sufficient to provide the attenuation above 100 dB in the stop band, as shown in Fig. 4(a) by the dark gray line.

The filter performance is nearly unchanged at T = 77.4 K, as shown in Fig. 4(b). The 3 dB cut-off frequency of the filter is increased to 7.0 MHz because the capacitance of the SMD capacitors was slightly reduced at 77.4 K. The deterioration of the attenuation at 1.4 and 3.1 GHz might be due to the shape resonances in the PCB boards, which can be eliminated by the proper profiling of the PCB edges. We used the same values of the inductances and capacitances for each pole of the LC filter, which resulted in ripples in the filter attenuation. These ripples can be reduced by the proper choice of inductances and capacitances, e.g., using the Butterworth filter design. The CPW-MP filters integrated with the LC

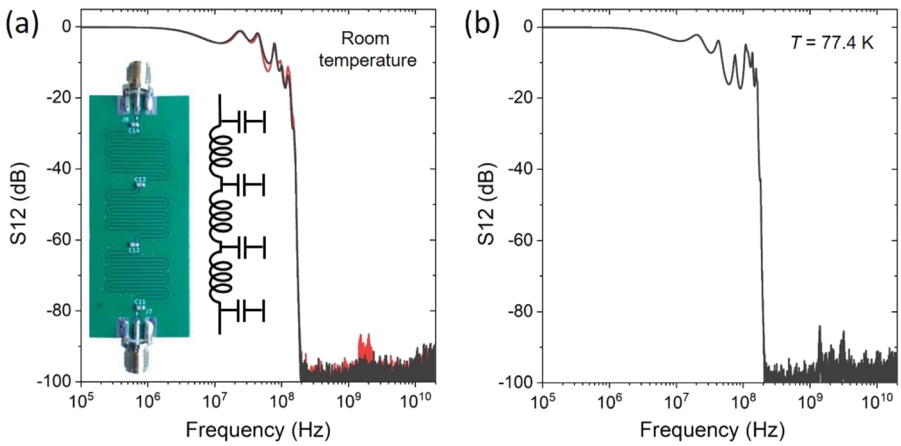

FIG. 4. Attenuation of a CPW-MP filter integrated with a 6-pole LC filter (a) at room temperature and (b) at T = 77.4 K. Inset in (a): the design and the circuit diagram of a 0.314 m-long CPW-MP filter integrated with the 3-pole LC filter. Red and gray lines show attenuation of filters with 0.641 and 0.848 m-long central tracks, respectively.

filter discussed in this section are impedance matched in the limited frequency range and possess an S11 parameter below −10 dB up to frequencies of 2.2–9.8 MHz, depending on the total filter capacitance (see the supplementary material).

D. Cryogenic and vacuum compatibility

The properties of the filter's absorption coating should not change after multiple thermal cycles. We performed a cryogenic shock test by immersing the filter in liquid nitrogen and then heating it to room temperature with a hot air gun. We found neither delamination nor cracks in the stainless steel powder absorption coating nor changes in the electrical properties of the filter, including the filter resistance and S11 and S12 parameters, after the ten thermal cycles (see the supplementary material for S11 and S12 parameters).

To prove the vacuum compatibility, we placed the CPW-MP filter without an aluminum foil shield inside the Tee vacuum fitting and evacuated it at room temperature using the MiniTask Pump Station (Agilent). A guard vacuum of 5×10^{-5} mbar was reached within 4.5 min, which qualifies the vacuum compatibility of the developed filters. Further improvements toward the ultra-high vacuum requirements can be made by replacing the self-adhesive silver foil with a metal layer deposited by sputtering or evaporation and the FR-4 PCB with a copper core or CuFlon PCB.

E. Integration with HDL-5 cryostat

Recently, we have demonstrated the energy-level quantization for the phase-slip $YBa_2Cu_3O_{7-x}$ (YBCO) nanowires with a crossover temperature between the thermal and quantum regimes of 12–13 K.[23] We consider these nanowires to be promising for the development of a superconducting qubit with a high operating temperature of a few K. As in the case of devices made of low-temperature superconductors, appropriate filtering of the transmission lines is required to keep the electronic temperature of the YBCO nanowires close to the base temperature of the cryostat and suppress the thermally activated transition between the discrete energy levels of the nanowire. Glattli *et al.*[11] determined this attenuation as

$$A = \frac{e^{hf/k_BT_s} - 1}{e^{hf/k_BT} - 1}, \tag{1}$$

where h is the Planck constant, f is the frequency, k_B is the Boltzmann constant, T is the sample temperature, and T_s is the temperature of the hot source. Using Eq. (1), we calculate the attenuation of the transmission line connecting room temperature with T_s = 300 K and cold parts of the experimental setup for two base temperatures T of 1.6 and 4.2 K, which can be achieved in conventional liquid helium cryostats. The results of the calculations are shown in Fig. 5(a) with light and dark blue lines. We would like to note that the required attenuation of the transmission lines for the device operating at 4.2 K is significantly smaller than that for the device with a 10 mK operating temperature (e.g., conventional superconducting qubit), which should exceed 470 dB at 10 GHz. The higher operating temperature of the YBCO nanowire simplifies the wiring.

Using the results presented above, we designed the 8-channel low-pass filter. The photo of the low-pass filter with and without stainless steel powder coating and the photo of the filter placed on the cold plate of the HDL-5 cryostat (Infrared Laboratories) are shown in Figs. 5(b)–5(d), respectively. The filter consists of two PCBs with two differential CPWs on each. Each PCB is placed in an individual compartment of the shielding housing made of gold-plated copper, which can be mounted on the cold plate of the HDL-5 cryostat. The 0.425 m-long differential CPW was integrated with the 5-stage LC filter. The filter compartments are filled with the stainless

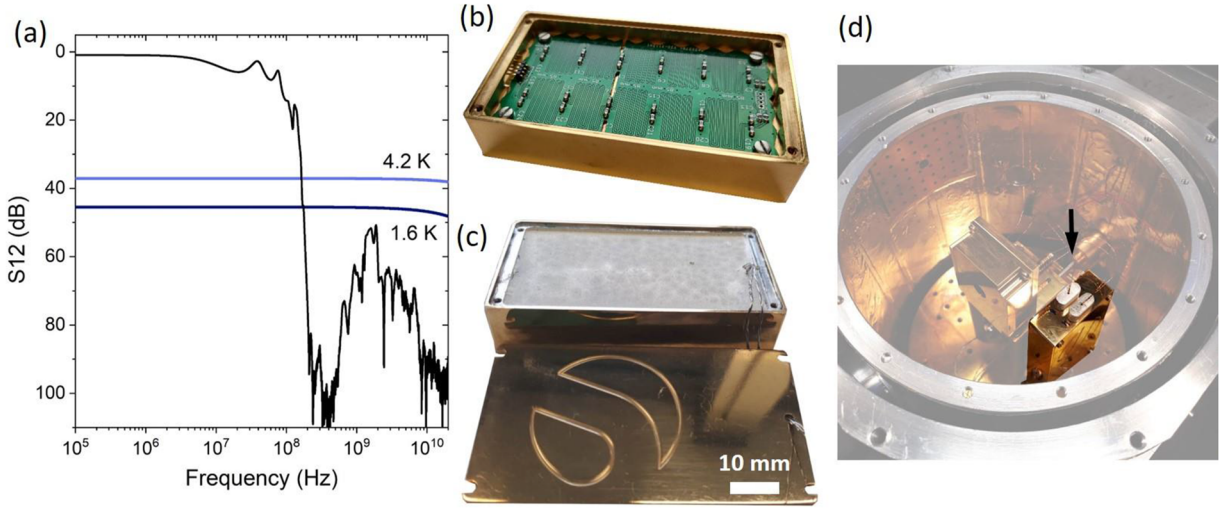

FIG. 5. (a) The required attenuation of the transmission line connecting room-temperature electronics and a device at two different base temperatures of 1.6 K (dark blue line) and 4.2 K (light blue line) from a room-temperature background and the measured S12 parameter of the CPW-MP filter at room temperature (black line). The photos of the 8-channel low-pass filter (b) without and (c) with stainless steel powder coating. (d) Photo of the CPW-MP filter integrated with HDL-5 cryostat. The filter is indicated by a black arrow. The 4 K radiation shield is not installed.

steel powder/VGE varnish coating. The surface of the stainless steel powder coating was covered with a 5 μm-thick silver layer deposited by the dc magnetron sputtering. The high-frequency performance of the filter was studied in a common mode. The ends of one wire of the differential pair were soldered to rigid coax cables with SMA connectors, while the ends of the second wire of the differential pair were grounded. The frequency dependence of the S12 parameter measured at room temperature is shown in Fig. 5(a) by a black line. The filter has a small attenuation of 0.9 dB at low frequencies due to a 10 Ω resistor connected in series with the CPW-MP filter and a 3 dB cut-off frequency of 10 MHz. The filter attenuation in the stop band (above 200 MHz) is above the theoretical estimates for the 1.6 and 4.2 K base temperatures, which confirms the proper filter design.

For the qubit measurements, the cryogenic low-pass filter has to provide adequate attenuation at frequencies above the plasma frequency of the superconducting nanowire qubit $f_p = (eI_c/\pi hC)^{1/2}$, which is of the order of several hundred GHz for the YBCO nanowires. Here, e is the elementary charge, and I_c and C are the critical current and capacitance of the nanowire, respectively. We calculate the required attenuation of the transmission line connecting room temperature and the devices cooled down to $T = 4.2$ K as 115 dB at frequencies up to 1 THz. Accurate measurements of the filter attenuation at such high frequencies are challenging. Therefore, we estimated the performance of the CPW-MP filter in the sub THz and THz ranges using the literature data. Cabello–Sánchez *et al.* measured an attenuation constant of CPW, α, between 0.68 and 0.99 mm^{-1} in the 750–1100 GHz frequency range, which provides an attenuation of 115 dB for the 13.4–19.5 mm-long CPW even without any absorption coating.[24] The radiation could also bypass the CPW through the FR4 dielectric. The loss tangent of the FR4 dielectric at 1 THz frequency is 0.13,[25] which corresponds to the attenuation constant $\alpha_{FR4} = 2.8$ mm^{-1}. The 115 dB attenuation at 1 THz is already achieved for the 9.7 mm-long PCB with FR4 dielectric. Taking into account the CPW length of 425 mm and the PCB length of 64 mm, the estimated attenuation of the fabricated CPW-MP filter at THz frequencies is well above 115 dB. We used PCBs with a conventional FR4 dielectric for filter fabrication because the optical and infrared components are filtered at the wiring stage. If the CPW-MP filter also has to attenuate the optical and infrared components, the black core FR4 dielectric should be used. From these estimates, we conclude that the fabricated CPW-MP filter should effectively attenuate the signals in the stop band.

The resistance of the 0.425 m-long CPW-MP filter is estimated at 1.1 Ω at 4 K. Taking into account the heat conductivity of the FR4 dielectric at cryogenic temperatures[26] and the CPW dimensions, we estimate an increase in the CPW-MP temperature due to the Joule heating by the 1 mA bias current as 0.2–0.7 mK in the 1.6–4.2 K temperature range, which is significantly smaller than the cryostat base temperature. For higher values of heat dissipation, the copper core PCB can provide better thermal anchoring at mK temperatures.

IV. CONCLUSIONS

We fabricated and characterized the impedance-matched CPW-MP low-pass filters for cryogenic measurements. The CPW-MP filter parameters can be tuned to meet experiment requirements using the measured values of the attenuation per length and the effective dielectric constant of the MP/VGE varnish coating. We integrated the CPW-MP filter with the multipole LC filter and achieved a low cut-off frequency, attenuation above 100 dB in the stop band, and a high roll-off of 590 dB per decade. The 8-channel low-pass filter was designed and integrated with the 4 K HDL-5 cryostat for further study of the quantum properties of the phase-slip YBCO nanowires.

SUPPLEMENTARY MATERIAL

The supplementary material contains data on the VNA calibration at room and cryogenic temperatures, a comparison of the S12 and S21 parameters of the CPW-MP filter, the S11 parameter of the CPW-MP filters integrated with a multistage LC filter, and the S-parameters of the CPW-MP filter before and after the thermal cycling test.

ACKNOWLEDGMENTS

I.G. was supported by the Deutsche Forschungsgemeinschaft (DFG, German Research Foundation) under Germany's Excellence Strategy—Cluster of Excellence Matter and Light for Quantum Computing (ML4Q), Grant No. EXC 2004/1 390534769.

AUTHOR DECLARATIONS

Conflict of Interest

The authors have no conflicts to disclose.

Author Contributions

Matvey Lyatti: Conceptualization (lead); Investigation (equal); Writing – original draft (lead); Writing – review & editing (equal). **Raphael Roth**: Investigation (equal); Writing – original draft (equal); Writing – review & editing (equal). **Irina Gundareva**: Investigation (equal); Writing – original draft (equal); Writing – review & editing (equal). **Detlev Grützmacher**: Funding acquisition (lead); Writing – original draft (supporting); Writing – review & editing (equal). **Thomas Schäpers**: Project administration (lead); Writing – original draft (equal); Writing – review & editing (equal).

DATA AVAILABILITY

The data that support the findings of this study are available from the corresponding author upon reasonable request.

REFERENCES

[1] J. M. Martinis, M. H. Devoret, and J. Clarke, Phys. Rev. B **35**(10), 4682–4698 (1987).
[2] A. Lukashenko and A. V. Ustinov, Rev. Sci. Instrum. **79**(1), 014701 (2008).
[3] F. Mueller, R. N. Schouten, M. Brauns, T. Gang, W. H. Lim, N. S. Lai, A. S. Dzurak, W. G. van der Wiel, and F. A. Zwanenburg, Rev. Sci. Instrum. **84**(4), 044706 (2013).
[4] F. P. Milliken, J. R. Rozen, G. A. Keefe, and R. H. Koch, Rev. Sci. Instrum. **78**(2), 024701 (2007).
[5] D. Vion, P. F. Orfila, P. Joyez, D. Esteve, and M. H. Devoret, J. Appl. Phys. **77**(6), 2519–2524 (1995).

[6]K. Bladh, D. Gunnarsson, E. Hurfeld, S. Devi, C. Kristoffersson, B. Smalander, S. Pehrson, T. Claeson, P. Delsing, and M. Taslakov, Rev. Sci. Instrum. **74**(3), 1323–1327 (2003).
[7]M. Thalmann, H. F. Pernau, C. Strunk, E. Scheer, and T. Pietsch, Rev. Sci. Instrum. **88**(11), 114703 (2017).
[8]D. Razmadze, D. Sabonis, F. K. Malinowski, G. C. Menard, S. Pauka, H. Nguyen, D. M. T. van Zanten, E. C. O'Farrell, J. Suter, P. Krogstrup, F. Kuemmeth, and C. M. Marcus, Phys. Rev. Appl. **11**(6), 064011 (2019).
[9]D. Sabonis, E. C. T. O'Farrell, D. Razmadze, D. M. T. van Zanten, J. Suter, P. Krogstrup, and C. M. Marcus, Appl. Phys. Lett. **115**(10), 102601 (2019).
[10]A. B. Zorin, Rev. Sci. Instrum. **66**(8), 4296–4300 (1995).
[11]D. C. Glattli, P. Jacques, A. Kumar, P. Pari, and L. Saminadayar, J. Appl. Phys. **81**(11), 7350–7356 (1997).
[12]E. J. Wollack, D. T. Chuss, K. Rostem, and K. U-Yen, Rev. Sci. Instrum. **85**(3), 034702 (2014).
[13]A. Paquette, J. Griesmar, G. Lavoie, R. Albert, F. Blanchet, A. Grimm, U. Martel, and M. Hofheinz, Appl. Phys. Lett. **121**(12), 124001 (2022).
[14]S. Danilin, J. Barbosa, M. Farage, Z. M. Zhao, X. B. Shang, J. Burnett, N. Ridler, C. Li, and M. Weides, EPJ Quantum Technol. **9**, 1 (2022).
[15]A. I. Ivanov, V. I. Polozov, V. V. Echeistov, A. A. Samoylov, E. I. Malevannaya, A. R. Matanin, N. S. Smirnov, and I. A. Rodionov, Appl. Phys. Lett. **123**(20), 204001 (2023).
[16]M. V. Moghaddam, C. W. S. Chang, I. Nsanzineza, A. M. Vadiraj, and C. M. Wilson, Appl. Phys. Lett. **115**(21), 213504 (2019).
[17]D. F. Santavicca and D. E. Prober, Meas. Sci. Technol. **19**(8), 087001 (2008).
[18]See https://www.lakeshore.com/products/categories/overview/temperature-products/cryogenic-accessories/varnish for information about VGE-7031 varnish.
[19]B. C. Wadell, *Transmission Line Design Handbook* (Artech House, Inc., Norwood, 1991).
[20]G. E. Conklin, Rev. Sci. Instrum. **36**, 1347–1349 (1965).
[21]M. J. Akhtar, N. K. Tiwari, J. Devi, M. Mahmoud, G. Link, and M. Thumm, Frequenz **68**(1–2), 69–81 (2014).
[22]F. Teyssandier and D. Prêle, in 9th International Workshop on Low Temperature Electronics (WOLTE9), Guaruja, Brazil, 2010.
[23]M. Lyatti, M. A. Wolff, I. Gundareva, M. Kruth, S. Ferrari, R. E. Dunin-Borkowski, and C. Schuck, Nat. Commun. **11**(1), 763 (2020).
[24]J. Cabello-Sánchez, H. Rodilla, V. Drakinskiy, and J. Stake, "Transmission loss in coplanar waveguide and planar Goubau line between 0.75 THz and 1.1 THz," in *43rd International Conference on Infrared, Millimeter, and Terahertz Waves (IRMMW-THz)* (IEEE, 2018), pp. 1–2.
[25]J. Carter, H. Lees, Q. G. J. Wang, S. J. Chen, S. Atakaramians, and W. Withayachumnakul, "Terahertz properties of common microwave dielectric materials," J. Infrared, Millimeter, Terahertz Waves **44**(11–12), 873–884 (2023).
[26]P. Duthil, CAS-CERN *Accelerator School: Superconductivity for Accelerators* edited by R. Bailey (Erice, Italy, 2013), 10.5170/CERN-2014-005.77.